Dynamics and Control 3, 261–280 (1993)

Vibration Control of a Two-Link Flexible Robot Arm

KENNETH L. HILLSLEY AND STEPHEN YURKOVICH
The Ohio State University, Department of Electrical Engineering, 2015 Neil Avenue, Columbus, Ohio 43210

Received September 11, 1991; revised August 11, 1992
Editor: M. Corless

Abstract. Analysis and experimentation is described for a two-link apparatus in which both members are very flexible. Attention is focused on endpoint position control for point-to-point movements, assuming a fixed reference frame for the base, with two rotary joints. Each link is instrumented with acceleration sensing and is driven by a separate motor equipped with velocity and position sensing. The control perspective adopted is to implement a two-stage control strategy in which the vibration control problem for fine-motion endpoint positioning is considered separate from the gross-motion, large-angle slew problem. In the first stage the control law shapes the actuator inputs *for the large-angle movement* in such a way that minimal energy is injected into the flexible modes, while in the second phase an endpoint acceleration feedback scheme is employed in independent joint control *for vibration suppression* at the link endpoints.

1. Overview

Despite the recent developments in experimental active vibration control for single-link flexible manipulators, relatively little activity has focused on the controller design for multilink flexible manipulators, and preliminary work has only recently begun to appear. While most experimental studies have focused on single-link manipulators, or multilink manipulators with a single flexible link, such setups have served as valuable testbeds for modeling, system identification, and controller design. Some of the more recent visible experimental efforts have been [1–10].

The classical literature abounds with works on the general topical area of coupled flexible bodies, and many of the more well-known books on the subject offer analytical developments for modeling such complex systems. Much less emphasis in the literature has been given to practical applications, however, and until the recent swelling of interest in flexible robotic systems very little has been reported for experimental work. The problem of endpoint position control of a multilink flexible robotic manipulator embodies much of the spirit of the generic multibody interaction problem, and the experimental nature of the robotics field in general, and particularly for this problem has added insight into the modeling and control problems at hand. References [11] and [12] discuss some of the modeling issues and offer several related references.

Controlling coupled flexible member systems remains an open problem, particularly from the implementation viewpoint. For this article, we focus our attention on the endpoint position control of a two-member system, assuming a fixed reference frame for the base, with two rotary joints. The control perspective we adopt is to implement a two-stage, or composite, control strategy in which the vibration control problem for fine-motion endpoint

positioning is considered separate from the gross-motion, large-angle slew problem. In the first stage, an input shaping scheme is used to alter the actuator inputs in such a way that minimal energy is injected into the flexible modes [13–17]. Such methods for slewing control seek to shape the input via convolution with a sequence of impulses, based on the idea that superposition of impulse responses can produce a movement with no vibrational motion after the input has ended. The contribution of this article along these lines is to incorporate the basic idea in combination with closed-loop control, combining endpoint acceleration feedback with joint information feedback.

The organization of this article is as follows. First, a description of the experimental apparatus is given, followed by a discussion of modeling and modal analysis. Following this, an implementation of input shaping is presented, with discussions on its limitations. A derivation of this prefiltering scheme in terms of a frequency-domain representation is given as an alternative to the time-domain interpretation appearing in [14]; for control purposes, much insight is gained via our representation. A relatively simple control design, based on a system linearization and employing acceleration feedback, is described next, and used in conjunction with the open-loop shaping scheme to improve system robustness to disturbances, nonlinear effects, and modeling uncertainties.

2. Hardware description

The apparatus considered in this work consists of two flexible links situated in the horizontal plane, as illustrated in Figure 1. This setup lends itself to complicated modeling as well as identification and control problems, not only from a robotics viewpoint but also from a multibody interaction viewpoint. A Motorola 68020/68881 system is the control computer for this setup.

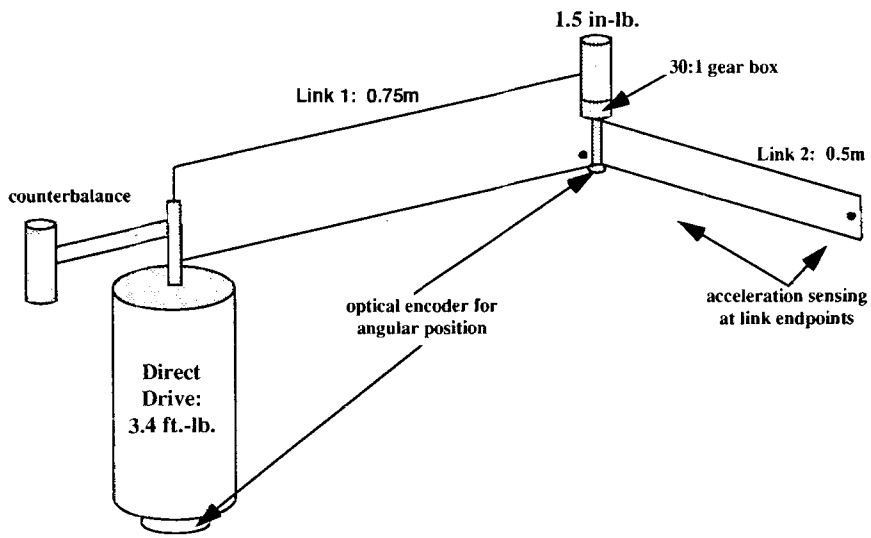

Figure 1. Two-link system.

The first link, which is driven by a 3.4-ft-lb direct drive servomotor, is 0.75 m long, 0.127 m high, and made of 2.3-mm-thick aluminum, with a counterweight centered about the motor axis for balance and protection of motor bearings. The servomotor is a six-pole, permanent-magnet, direct-current motor with a rated stall torque of 4.802 N-m (680 oz-in), manufactured by the Inertial Motor Corporation. The linear power amplifier available for this motor from the same manufacturer is an analog amplifier that closes a velocity loop with the motor, essentially providing the user with a nearly linear device, with characteristics of a low-pass filter.

Mounted at the endpoint of the first link is a geared servomotor to actuate the smaller (0.5 m long, 0.038 m high) second link made of 1-mm-thick aluminum. The joint, which was designed and built in-house, consists of a free rotating hub set between two bearings, allowing approximately $\pm 170°$ rotation. The motor and optical encoder are mounted above and below, respectively. The motor is manufactured by Electro-Craft, Inc., with a rated stall torque of 2.5 oz-in. With the gearhead, 30:1 ratio with maximum speed of 250 rpm, the gearmotor produces a maximum torque of 1.5 lb-in. The motor and gearhead combination is less than 4 in long and weighs approximately 12 oz, so that the total weight of the joint is less than 1.5 lb. Like the larger motor, an analog amplifier (modular controller card) accompanies the gearmotor, and a local velocity loop is closed around the motor. The links are interchangeable with several others of varying thicknesses, lengths, and flexibility.

Built in to the large motor housing of the first joint is an 1800-line quadrature shaft encoder used to detect the angular displacement of the motor shaft. At the second joint (smaller motor), an externally mounted optical encoder is used. Presently, a device from BEI Motion Systems, Inc. is used, which has a resolution of 500 pulses per revolution. As alluded to above, both joints have colocated velocity sensing for analog feedback as well as for digital control using shaft velocities. Lightweight acceleromters (6.7 g in a 0.56-in round casing) are mounted at the endpoint of each link for measuring linear acceleration. These devices are PiezoBEAM^{TM} accelerometers from the Kistler Instrument Corporation, and incorporate a zirconate titanate bimorph piezoelectric sensing element. The acceleration range is ± 5 g, with an acceleration limit of ± 8 g, and the sensitivity (at 100 Hz) is about 1 volt/g. Additional sensing for data recording (not used in feedback control) is provided by a linear-array line scan camera to record endpoint position. The relatively small field of view of the camera limits its usefulness for large-angle motions; for this reason, results are typically displayed for the final phase of the overall motion.

3. Modeling and modal analysis

3.1. Uncoupled system

The two-link flexible manipulator can be considered to be a pair of uncoupled links under (extreme) constrained conditions. For example, interaction between the two links is minimal when the forearm link moves while the upper arm is stationary, or when the upper arm link moves while the forearm link is locked at 90^0 (measured as the angle between the two links).

Initial experiments were performed to determine the modes of vibration of the uncoupled-link system; that is, to determine the modes of vibration of the individual links. To determine the upper-arm-link vibrational modes, a pulse voltage was applied to the upper arm actuator while the forearm was locked (with an externally mounted metal bracket) at 90°. Similarly, to determine the forearm-link vibrational modes, a pulse voltage was applied to the forearm actuator while the upper arm was kept stationary. The frequency spectrums of the pulse inputs were such that all frequencies below 6 Hz were sufficiently excited.

Using a sampling period of 0.02 second, 512 acceleration data points were collected and filtered by an eighth-order Butterworth filter with a 7 Hz cutoff frequency. 1024-point FFT operations were performed on the data (zero padded to reduce the spacing between frequency samples) to determine the frequency content. FFT plots of the acceleration signals are shown in figure 2, and indicate an approximate 1.2 Hz upper arm damped natural frequency and an approximate 2.5 Hz forearm damped natural frequency. Hence, each link exhibits a single dominant mode of vibration. Neither link exhibits significant spectrum amplitudes corresponding to higher frequency modes.

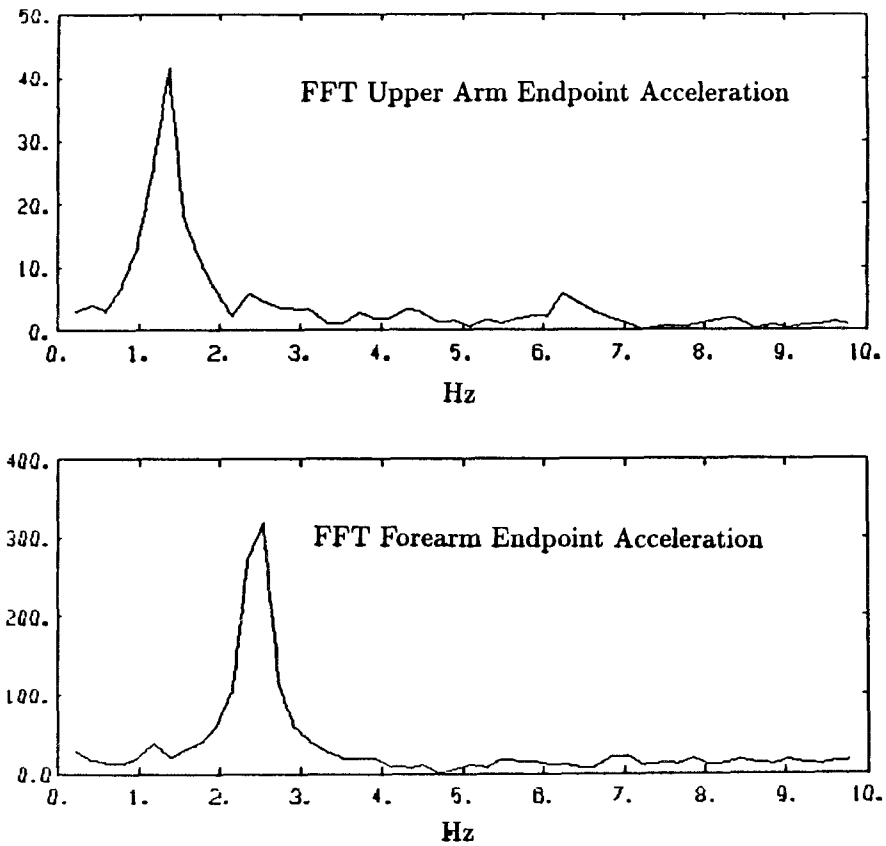

Figure 2. Uncoupled system damped natural frequencies.

3.2. *Coupled system*

It is well known that such mechanical systems, in most useful configurations, experience a great deal of coupling between the flexible members, and this is verified in the experimental apparatus of this study. For example, when the links undergo simultaneous movements or when the forearm link is locked at an angle larger than 90° between the two links, there is a strong interaction of flexible modes between the two links, and the links are considered to be coupled.

The next set of experiments were performed to determine the flexible modes of the coupled-link system. In the first experiment, pulse voltages were applied to the upper arm and forearm actuators simultaneously resulting in a 20° slew of each link. The upper arm was initially positioned at 0° relative to a fixed frame of reference. The forearm was initially positioned at −10° (positive angle measured clockwise relative to upper arm).

FFT plots of the two endpoint accelerations appear in figure 3, and illustrate the strong coupling of flexible modes between the links. The 1.2 Hz mode from the upper arm appears in the forearm, while the 2.5 Hz mode from the forearm appears in the upper arm.

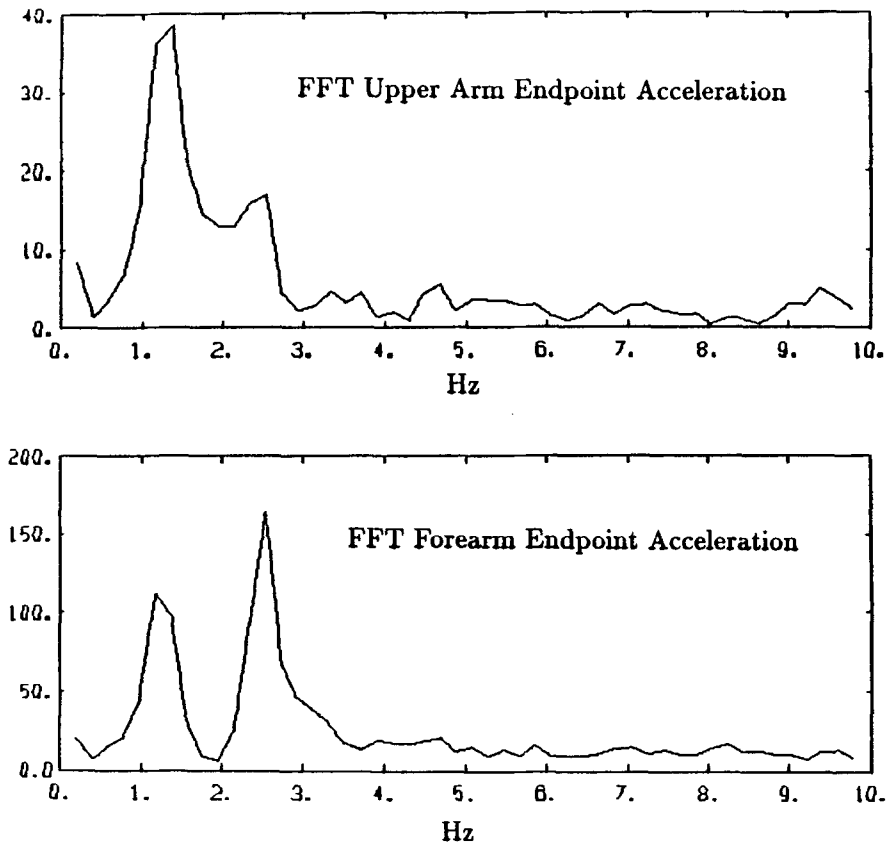

Figure 3. Coupled system damped natural frequencies.

Investigating further the frequencies of the flexible modes, a series of experiments were performed in which a voltage was applied to the upper arm actuator with the forearm link locked at various angles. The forearm link was locked at four different angles (measured as the angle between the upper arm and forearm link): 180°, 135°, 90°, and 45°. For each configuration, a pulse voltage was applied to the upper arm actuator resulting in a 20° slew of the system, and endpoint acceleration data were collected from the upper arm and forearm endpoints.

As indicated in table 1, the upper arm has a 1.074 Hz mode of vibration for the case in which the two links are 180° apart. The frequency of this mode increases from 1.074 Hz to 1.172 Hz as the angle between the two links decreases from 180° to 45°. This result is to be expected, since the mass moment of inertia with respect to the upper arm actuator decreases with the decrease in angle. As seen from the upper arm actuator, the effective load decreases leading to the increase in frequency of vibration. The forearm mode of vibration, on the other hand, *decreases* from 2.588 Hz to 2.344 Hz. Thus, the configuration of the two links has a significant effect on the frequency of the forearm mode.

Based on the movement of the frequencies of the flexible modes and the coupling of the modes, a hypothesis of the two-link flexible body dynamics can be formed suggesting that in a coupled movement the system can be considered to consist of superimposed power-varying and frequency-varying modes of vibration. This is in agreement with the well-known theory of coupled multiple bodies, which will not be repeated here; more discussion appears in [12].

4. Input shaping control

One objective of control for the two-link flexilbe manipulator is to achieve accurate, steady forearm endpoint position after the manipulator executes a point-to-point movement. Methods for control of vibrations in flexible link manipulators traditionally have focused on damping vibrations that result when control is applied. A different method for vibrational controls is input shaping.

4.1. Background

Input shaping is an open-loop compensator that alters (shapes) the actuator input such that vibrational motion is eliminated after the input has ended. The method is based on the notion that superimposed impulse responses can exactly cancel one another after the last impulse.

Table 1. Upper arm and forearm damped natural frequencies.

	Locked angle between links			
Link	180°	135°	90°	45°
Upper arm (Hz)	1.074	1.074	1.123	1.172
Forearm (Hz)	2.588	2.539	2.393	2.344

Implementing input shaping control involves convolving a sequence of impulses with the reference inputs. The critical parameters of the scheme are the amplitudes and application times of the impulses. Impulse amplitudes are a function of modal damping, and application times are a function of modal damping and frequency. An important assumption of input shaping control is that the frequencies and dampings of the modes of vibration are known a priori. Note that numerator dynamics of the system (zeros) are not considered in designing an impulse sequence.

In [14] it is argued that elimination of vibration after the input has ended requires that an expression for the amplitude of vibration equal zero at the instant the input ends. Relationships for impulse amplitudes and application times in terms of modal damping and frequency are fomulated from this requirement.

From a different perspective, the action of adding an appropriately delayed impulse response to another impulse response is, essentially, to add zeros to the system function at the exact locations of the system modes (poles). To see this fact, assume that the system consists of a pair of complex poles located in the complex s-plane at $s = -\sigma \pm j\omega$. Letting $h(t)$ denote the system impulse response, if an impulse sequence $u(t) = \alpha_0\delta(t) + \alpha_1\delta(t - t_1)$ is input to the system, the Laplace transform of the output will be

$$\begin{aligned} Y(s) &= \alpha_0 H(s) + \alpha_1 \exp^{-st_1} H(s) \\ &= H(s)(\alpha_0 + \alpha_1 \exp^{-st_1}), \end{aligned} \tag{1}$$

and it is evident that multiple pairs of complex zeros are introduced to the system function.

Setting $\alpha_0/\alpha_1 + \exp^{st_1} = 0$, and setting the location of the fundamental pair of complex zeros contributed by the shaped input equal to the exact location of the pair of complex system poles, $s = -\sigma \pm j\omega$, results in

$$\frac{\alpha_0}{\alpha_1} = -\exp^{\sigma t_1} \exp^{\pm j\omega t_1}. \tag{2}$$

The application time, t_1, of the second impulse and the amplitudes of the two impulses, α_0 and α_1, can be expressed in terms of the pole (and zero) location in the s-plane. Specifically, the application time, t_1, is determined from

$$\exp^{\pm j\omega t_1} = -1. \tag{3}$$

Hence,

$$t_1 = \frac{\pi}{\omega}, \tag{4}$$

where ω is the damped natural frequency of the system poles in question. Thus, in terms of the undamped natural frequency, ω_n, the impulse application time is expressed as

$$t_1 = \frac{\pi}{\omega_n \sqrt{1 - \zeta^2}}. \tag{5}$$

The impulse amplitudes, α_0 and α_1, are determined by first noting that the damping ratio, ζ, of the system poles can be expressed as σ/ω_n. Substituting $\omega_n \zeta$ for σ and the above expression for t_1 into

$$\frac{\alpha_0}{\alpha_1} = \exp^{\sigma t_1}, \tag{6}$$

results in

$$\frac{\alpha_0}{\alpha_1} = \exp^{\frac{\zeta\pi}{\sqrt{1-\zeta^2}}}. \tag{7}$$

Imposing the constraint $\alpha_0 + \alpha_1 = 1$ on the impulse amplitudes to ensure that the shaped input voltage has the same energy as the reference voltage, and solving for α_0 and α_1, results in

$$\alpha_0 = \frac{1}{1 + \exp^{\frac{-\zeta\pi}{\sqrt{1-\zeta^2}}}}, \tag{8}$$

$$\alpha_1 = \frac{\exp^{\frac{-\zeta\pi}{\sqrt{1-\zeta^2}}}}{1 + \exp^{\frac{-\zeta\pi}{\sqrt{1-\zeta^2}}}}. \tag{9}$$

Thus, if impulses of amplitude α_0 and α_1, and corresponding application times 0 and t_1, as specified above, are applied to the system, the complex system poles will be exactly cancelled with zeros.

If the locations of the system poles are not known precisely, vibrations will not be completely eliminated after the input has ended. To increase robustness to uncertainty in frequency and damping of the system poles, a three-impulse sequence can be used. In [14], the additional impulse to the sequence is needed to satisfy an additional constraint on the system that the derivative with respect to frequency of an expression for the amplitude of vibration be set equal to zero. Essentially, this constraint states that residual vibrations of the system are to change little with respect to changes in natural frequency.

A different perspective of the increased robustness in terms of pole-zero cancellation is described in the following analysis. When three impulses with proper amplitude are applied to the system at the appropriate times, two pairs of complex zeros, rather than one, are added to the system function at the exact location of the pair of complex poles. Robustness to system uncertainty is improved, since there are two zeros in the vicinity of each complex pole rather than one.

Again, assuming that the system consists of a pair of complex poles located in the complex s-plane at $s = -\sigma \pm j\omega$, and letting $h(t)$ denote the system impulse response, if an impulse sequence $u(t) = \alpha_0\delta(t) + \alpha_1\delta(t - t_1) + \alpha_2\delta(t - t_2)$ is input to the system, the Laplace transform of the output will be

$$\begin{aligned} Y(s) &= \alpha_0 H(s) + \alpha_1 \exp^{-st_1} H(s) + \alpha_2 \exp^{-st_2} H(s) \\ &= H(s)(\alpha_0 + \alpha_1 \exp^{-st_1} + \alpha_2 \exp^{-st_2}). \end{aligned} \tag{10}$$

If the two fundamental pairs of complex zeros are to coincide exactly with the pair of system complex poles, the equation

$$\alpha_0 + \alpha_1 \exp^{-st_1} + \alpha_2 \exp^{-st_2} = 0 \tag{11}$$

must be factorable into the form

$$(\phi + \psi \exp^{-st_1})^2 = 0, \tag{12}$$

where, as in the two-impulse sequence, $s = -\sigma \pm j\omega$ is the location of the pair of system complex poles.

The impulse amplitudes, ϕ, ψ, and second-impulse application time, t_1, above were found in the two-impulse analysis to be

$$t_1 = \frac{\pi}{\omega_n \sqrt{1 - \zeta^2}}, \tag{13}$$

$$\phi = \frac{1}{1 + \exp^{\frac{-\zeta\pi}{\sqrt{1-\zeta^2}}}}, \tag{14}$$

$$\psi = \frac{\exp^{\frac{-\zeta\pi}{\sqrt{1-\zeta^2}}}}{1 + \exp^{\frac{-\zeta\pi}{\sqrt{1-\zeta^2}}}}. \tag{15}$$

The impulse amplitudes and application times of the three-impulse sequence can be expressed in terms of ϕ, ψ, t_1 as follows: $t_2 = 2t_1$, $\alpha_0 = \phi^2$, $\alpha_1 = 2\phi\psi$, and $\alpha_2 = \psi^2$. Hence,

$$t_1 = \frac{\pi}{\omega_n \sqrt{1 - \zeta^2}}, \tag{16}$$

$$t_2 = \frac{2\pi}{\omega_n \sqrt{1 - \zeta^2}}, \tag{17}$$

$$\alpha_0 = \frac{1}{1 + 2\exp^{\frac{-\zeta\pi}{\sqrt{1-\zeta^2}}} + \exp^{\frac{-2\zeta\pi}{\sqrt{1-\zeta^2}}}}, \tag{18}$$

$$\alpha_1 = \frac{2\exp^{\frac{-\zeta\pi}{\sqrt{1-\zeta^2}}}}{1 + 2\exp^{\frac{-\zeta\pi}{\sqrt{1-\zeta^2}}} + \exp^{\frac{-2\zeta\pi}{\sqrt{1-\zeta^2}}}}, \tag{19}$$

$$\alpha_2 = \frac{\exp^{\frac{-2\zeta\pi}{\sqrt{1-\zeta^2}}}}{1 + 2\exp^{\frac{-\zeta\pi}{\sqrt{1-\zeta^2}}} + \exp^{\frac{-2\zeta\pi}{\sqrt{1-\zeta^2}}}}. \tag{20}$$

Note that, as in the two-impulse sequence, the sum of impulse amplitudes equals one.

Thus, if impulses of amplitude α_0, α_1, α_2, and application times 0, t_1, t_2, respectively, as specified above, are applied to a system in which the location of the pair of complex system poles is known exactly ($s = -\sigma \pm j\omega$), the pair of complex poles will be cancelled exactly with two pairs of complex zeros. If the locations of the poles are not known precisely, residual vibrations will change little.

Adding more impulses to the sequence introduces more pairs of complex zeros to the system function at the locations of the system poles. It should be noted, however, that adding more impulses adds lag to the system. Thus, there is a trade-off between robustness and speed of the system response.

In the preceding analysis, the equations for impulse amplitudes and application times were found for sequences of two and three impulses. In the more general case in which a sequence consists of N impulses, the impulse amplitudes and application times are given by

$$\alpha_{j-1} = \frac{\binom{N-1}{j-1}\exp^{-\frac{(j-1)\zeta\pi}{\sqrt{1-\zeta^2}}}}{\Sigma_{k=0}^{N-1}\binom{N-1}{k}\exp^{-\frac{k\zeta\pi}{\sqrt{1-\zeta^2}}}}, \quad j = 1, \ldots N \tag{21}$$

$$t_{j-1} = (j-1)\frac{\pi}{\omega_n\sqrt{1-\zeta^2}}, \quad j = 1, \ldots, N \tag{22}$$

where, again, ω_n is the undamped natural frequency, ζ is the corresponding damping ratio, and j is the index of impulses in the sequence.

To shape an input for more than one vibrational mode, an impulse sequence is designed for each mode individually. These sequences are then convolved together to form a new impulse sequence that is convolved with the reference input. For example, considering two modes of vibration and a two-impulse sequence for each mode, the new impulse sequence takes the form

$$[\alpha_0\delta(t) + \alpha_1\delta(t - t_a)] \star [\beta_0\delta(t) + \beta_1\delta(t - t_b)] =$$
$$\alpha_0\beta_0\delta(t) + \alpha_1\beta_0\delta(t - t_a) + \alpha_0\beta_1\delta(t - t_b) + \alpha_1\beta_1\delta(t - (t_a + t_b)), \quad (23)$$

where $\star$ denotes the convolution operation.

4.2. *Small-angle movement results*

Experiments in which the two links move through small angles (under 45°), and move in the same direction are described in this section. As previously noted, the frequencies of the modes of vibration depend greatly on the configuration of the two links. During small-angle movements in which the configuration of the links does not change significantly, the frequencies of the vibrational modes do not change significantly.

A no-control experiment was initially performed to establish a basis for comparisons with control experiments. Pulse voltages were applied to the two actuators, resulting in an approximate 20° slew of each link. The upper arm was initially positioned at 0°, and the forearm at −10°. The forearm endpoint position response for the no-control case is shown in figure 4, and illustrates the flexibility of the links. Note that in this plot and those to follow, the position as read by the camera is started at some time instant *after*

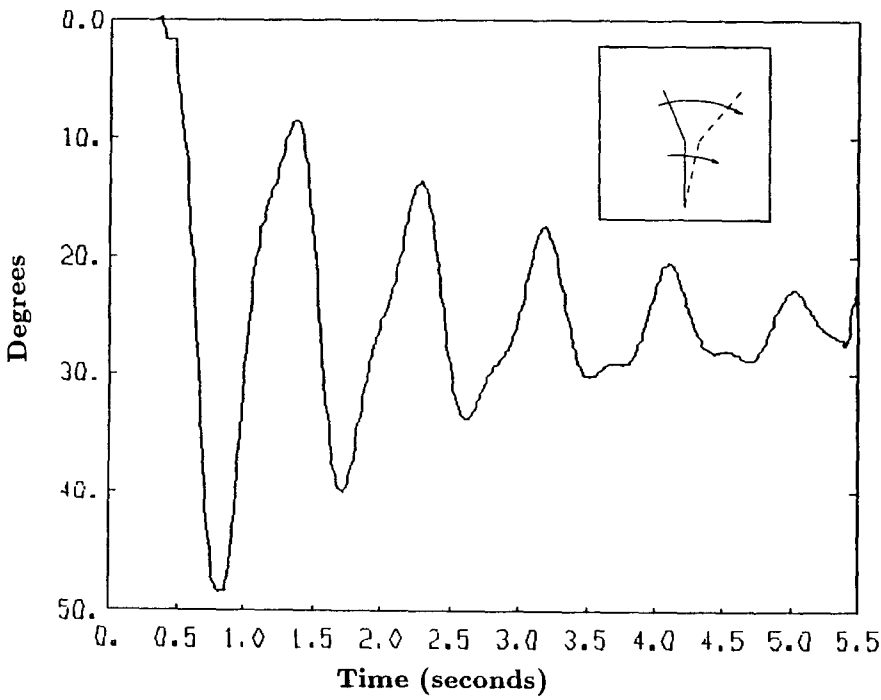

Figure 4. Forearm endpoint position with no control applied.

zero on the time axis. Also, because the field of view of the camera is only approximately 50°, all experiments are performed such that only the final portion of the movement is recorded by the camera.

In the initial control experiment, input shaping was implemented for independent joint control. A two-impulse sequence, designed for the 1.2 Hz vibrational mode of the upper arm, was convolved with the upper arm reference input. Similarly, a two-impulse sequence, designed for the 2.5 Hz mode of the forearm, was convolved with the forearm reference input. The damping ratios of the upper arm and forearm flexible modes (0.11 and 0.065, respectively) were determined empirically. The upper arm and forearm reference inputs and initial link configuration were identical to those in the no-control experiment (figure 4). The resulting forearm endpoint position is shown in figure 5. Although the response has less overshoot than the no-control response, the control is clearly ineffective in eliminating vibration of the 2.5 Hz component.

As previously discussed, during the movement in which the two links move simultaneously, the vibrational mode from one link appears in the other link as well, implying a coupling of vibrational modes. To improve endpoint position response, the coupling must be taken into account.

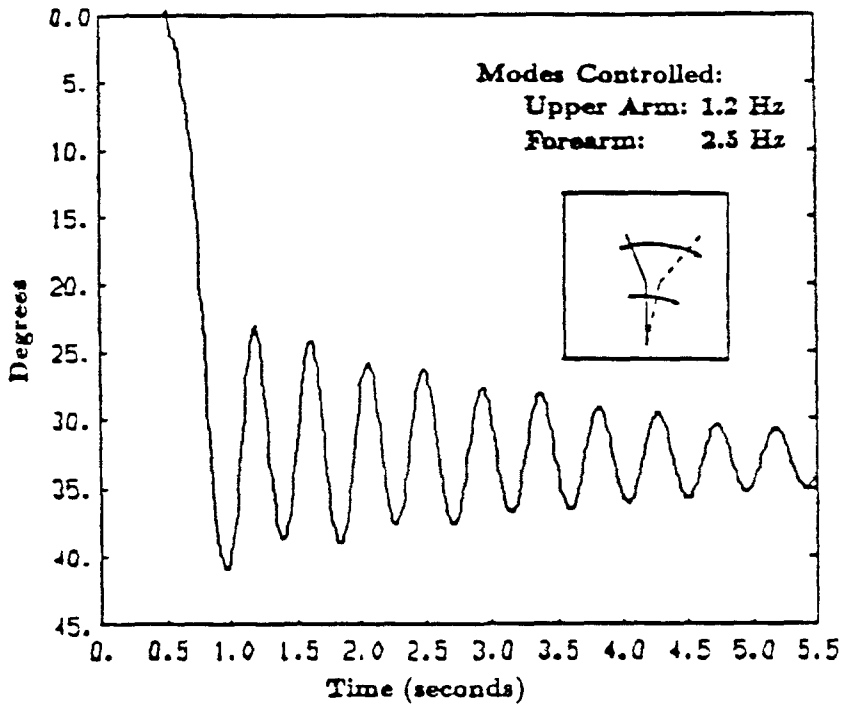

Figure 5. Forearm endpoint position with input shaping control.

In general, to control the two vibrational modes in each link, a two-impulse sequence is designed for each mode individually. Then, the two sequences are convolved together to form a four-impulse sequence that is convolved with each of the reference inputs. In this experiment, the upper arm and forearm reference inputs and initial configuration of the links are the same as in earlier experiments. The forearm endpoint position is shown in figure 6. The completely vibrationless response is evidence that controlling the coupled vibrational mode in each link is necessary.

4.3. Shortcomings

The most obvious shortcoming of an input-shaping precompensation scheme *alone* is its open loop nature. That is, with such a scheme there is essentially no robustness to external disturbances, and little effective robustness to modeling uncertainties.

On the other hand, input shaping control was shown to be an effective method for eliminating vibrational motion in small-angle movements, primarily because the frequencies of the vibrational modes do not vary greatly during the course of motion. Therefore, it is possible to design impulse sequences for nominal operating point frequencies. For larger-angle movements, however, the frequencies of the modes of vibration can vary

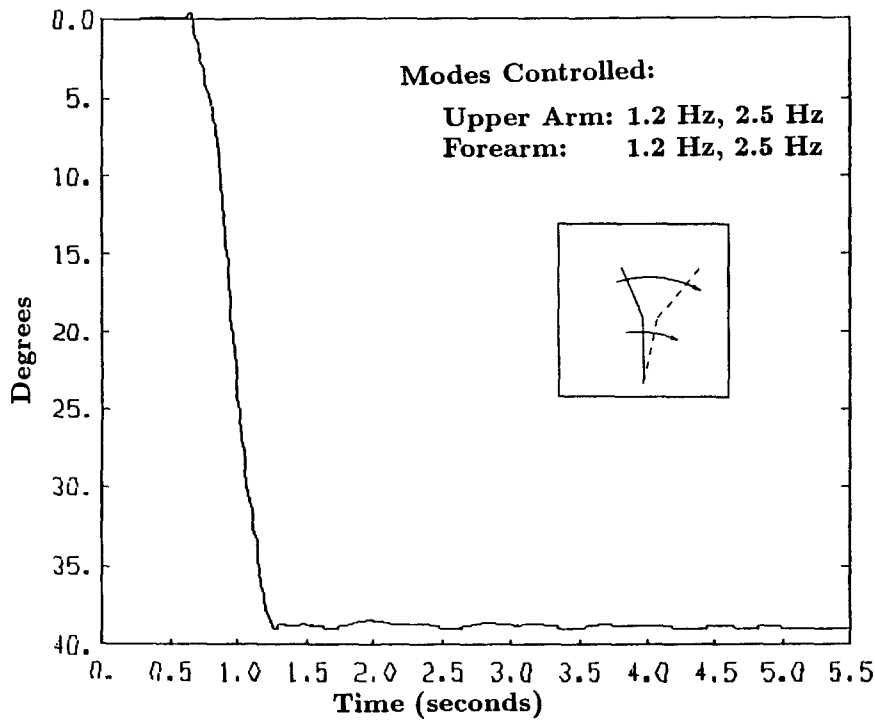

Figure 6. Forearm endpoint position with input shaping control.

significantly. As a result, impulse sequences cannot be designed to eliminate single-frequency vibrations. To illustrate the inability of input shaping to eliminate vibrational motion in movements in which the two links move at least 45°, an experiment was performed. The resulting shaped actuator profile slewed the upper arm link 45° and the forearm link 90°. The forearm endpoint position is shown in figure 7, and clearly indicates residual vibrations.

Because the input shaping algorithm is implemented on a digital computer, error is introduced due to sampling. The input shaping algorithm is digitally implemented by simply checking at each sampling instant the elapsed time and comparing it to the shaped input profile to determine the appropriate voltage to apply to the actuators. Two different approaches may be taken in approximating the ideal analog shaped input profile. The first approach is to leave the profile breakpoints (time instants at which the profile has a change in amplitude) unchanged from the ideal analog profile. Essentially, this approach performs a truncate operation in terms of signal application times, and the error is bounded by the sampling interval. A better approach is to round the breakpoints in the profile to the closest sampling time instant. This technique reduces the bound on the error to half the sampling interval.

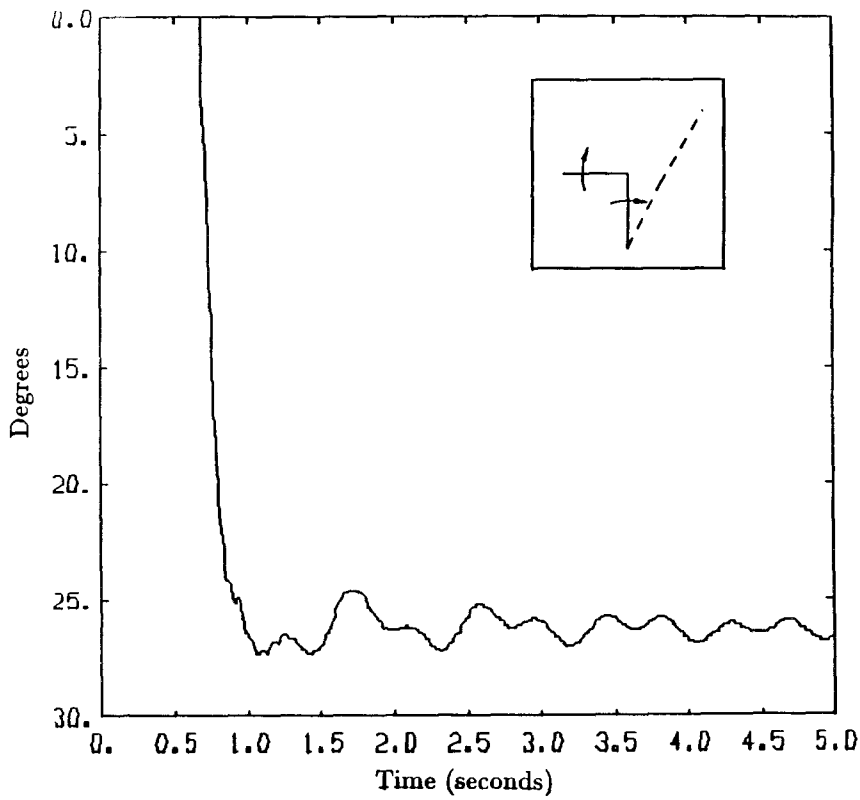

Figure 7. Input shaping control for a large-angle movement.

5. Combined feedforward and feedback control

5.1. Feedback control alone

Shaft position/endpoint acceleration feedback proportional control was demonstrated to be successful in eliminating endpoint vibrations of a single-link flexible manipulator [19]. For this multilink system, link endpoint acceleration data (filtered by an eighth-order Butterworth filter with a 7 Hz cutoff frequency) and actuator shaft position data from the two links are subtracted from reference values to form error signals. These error signals are then multiplied by appropriate gains and added together to form control inputs to the two actuators:

$$u_1(k) = K_{p1}(\theta_1^d - \theta_1(k)) - K_{a1}\alpha_1(k), \tag{24}$$

$$u_2(k) = K_{p2}(\theta_2^d - \theta_2(k)) - K_{a2}\alpha_2(k), \tag{25}$$

where $u_i(k)$ are the control inputs, θ_i^d are the desired actuator shaft positions, $\theta_i(k)$ are the measured actuator (and filtered) link endpoint accelerations, and K_{pi}, K_{ai} are the shaft position and endpoint acceleration feedback gains, respectively. We note that higher-order dynamics in the compensators have been added, with no appreciable improvement in performance; thus, in order to maintain a simple yet effective scheme, the above control law has been employed.

The method is decentralized in the sense that only local information from each link is used to form actuator control signals. For example, forearm actuator shaft position and link endpoint acceleration data are used in determining the forearm control signal. The shaft position feedback part of the structure is used to control rigid body motion, while the endpoint acceleration feedback part is used to control flexible body motion.

To determine appropriate feedback gains for each actuator input, a linear model is assumed for each transfer function from motor inputs to shaft angles and motor inputs to endpoint accelerations. This assumption is justifiable for small motions *after* the large-angle motion, particularly when the resulting control design is used in conjunction with an input shaping scheme in which minimal residual vibrations result from the large-angle motion. Hence, simple techniques considering the system pole-zero patterns (root locus design), or Ziegler–Nichols tuning rules, may be undertaken, and the resulting gains tuned empirically if necessary. That is, with the upper arm link stationary at 0° and the forearm endpoint acceleration gain set to 0, the shaft position feedback gain was determined by selecting the gain that produced the optimal response in terms of speed of response and (under)overshoot. Once the shaft position gain was determined, the endpoint acceleration gain was determined by selecting the gain that minimized vibrational motion. This procedure was repeated for the upper arm link with the forearm link locked at 90°. Feedback gains that were determined as described above for the uncoupled system were also used for control of the two links in coupled movements. It is important to note, of course, that due to the nonminimum-phase nature of the plant under control (because of noncolocated sensor/actuator pairs and the coordinate system used), care must be taken in the compensator design to avoid the use of high gains in the feedback.

To illustrate the performance of shaft position–endpoint acceleration feedback in damping vibrations after large angle movements, a pair of experiments was performed in which the upper arm was commanded to move 45° while the forearm was commanded to move 90° with the two links ending in the fully extended configuration. In both experiments, the upper arm and forearm endpoint acceleration feedback gains were $K_{a1} = -0.04$ and $K_{a2} = -0.1$, respectively, while upper arm and forearm shaft position feedback gains were $K_{p1} = 0.0025$, $K_{p2} = 0.01$ in one experiment, and $K_{p1} = 0.002$, $K_{p2} = 0.008$ in the other. The forearm endpoint position in figure 8 shows that vibrations are completely damped in a settling time of 2.25 seconds. As previously noted, decreasing the shaft position gains reduces the large fluctuations in the response, but also slows the response.

5.2. *Feedback control with input shaping*

Although shaft position-endpoint acceleration feedback control is effective in damping endpoint vibrations in large-angle movements, the scheme exhibits a trade-off between speed

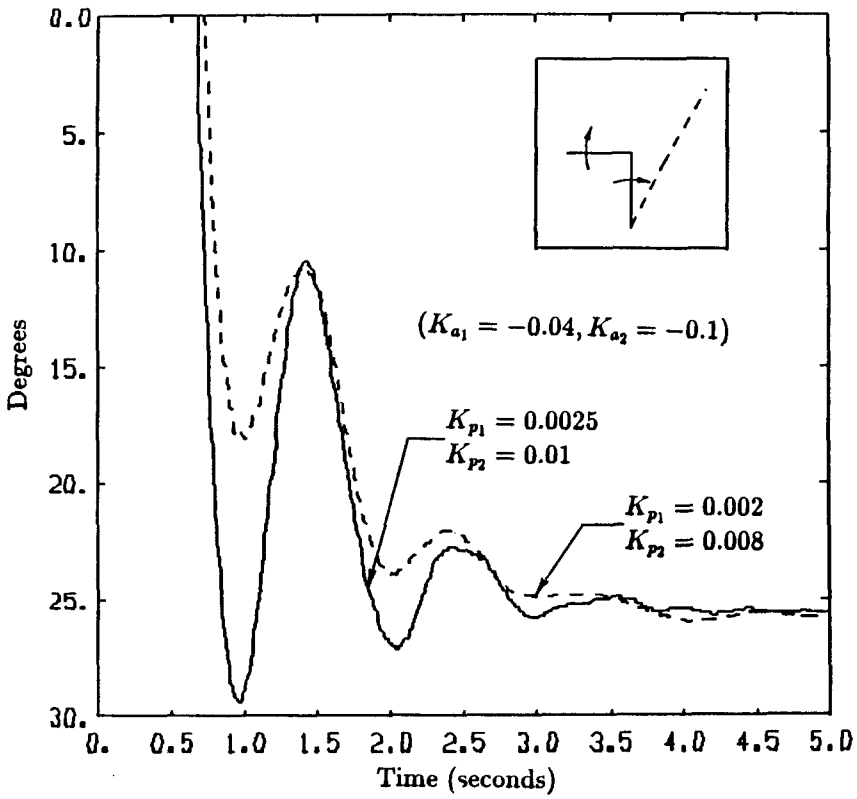

Figure 8. Endpoint acceleration feedback for a large-angle movement.

of response and (under)overshoot. Reducing shaft position feedback gains decreases the amplitude of the initial damped oscillations, but also slows the system response. Moreover, because the post-slew vibration suppression design is based on a linear model assumption for small motions, large residual vibrations following the gross-motion slew degrade the performance.

A different approach for controlling vibrations in large-angle movements, which considerably reduces (under)overshoot while maintaining speed of response, uses input shaping in conjunction with a post-slew feedback scheme (figure 9). Input shaping, in which the impulse sequences are designed for a nominal operating frequency, is used to move the links rapidly to the desired location with minimal residual vibration. Then, shaft position–endpoint acceleration feedback is used to dampen vibrations and maintain accurate forearm endpoint position. This composite control method enjoys the rapid rise time of input shaping control and vibration suppression of feedback control for large-angle movements while significantly reducing the large (under)overshoot exhibited in the feedback scheme of the preceding section.

As depicted in figure 9, the input-shaped voltage profiles are initially sent to the link actuators. These profiles move the manipulator to the desired configuration with minimal residual vibration. The two actuator inputs are shaped according to nominal flexible mode frequencies, such as the median frequencies of the range of frequencies covered during such a movement. At the instant in time when the shaped profiles end, $t = T$, control is switched to shaft position–endpoint acceleration feedback for closed-loop control damping of residual endpoint vibrations.

To illustrate the effectiveness of composite control, a set of experiments was performed comparing three different control schemes: composite, input shaping, and shaft position–endpoint acceleration feedback. The upper arm was commanded to slew 45°, and the forearm was commanded to slew 90°. A two-impulse sequence was designed for the 1.07 Hz (0.11 damping ratio) and 2.33 Hz (0.065 damping ratio) modes of vibration. The upper arm feedback gains were $K_{p1} = 0.0025$, $K_{a1} = -0.04$; the forearm feedback gains were $K_{p2} = 0.01$, $K_{a2} = -0.1$. The forearm endpoint position for the three methods is shown in figure 10.

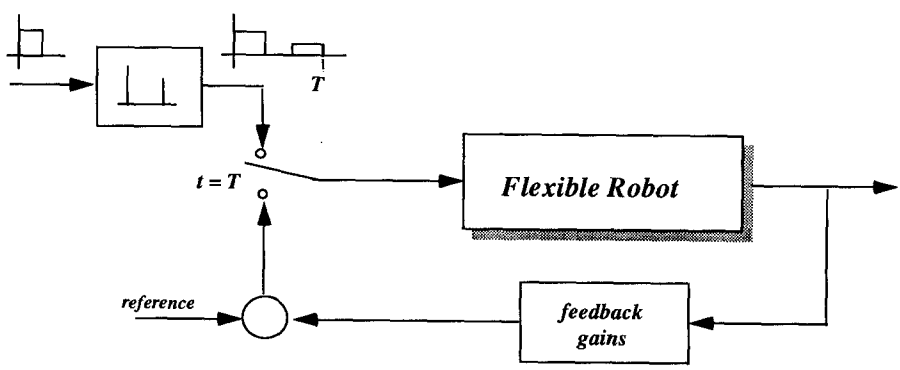

Figure 9. Composite control: input shaping and feedback.

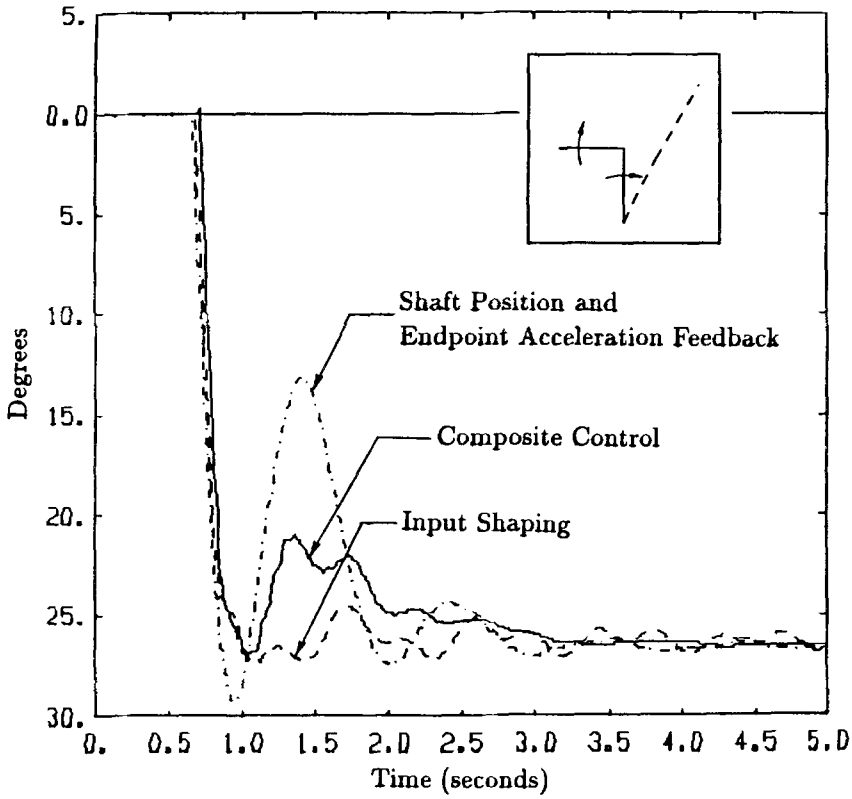

Figure 10. Composite control for a large-angle movement.

Shaft position–endpoint acceleration feedback dampens the vibrations in a settling time of 2.5 seconds, but exhibits a large undershoot (16 °). Input shaping shows very little undershoot, but results in residual vibrations. Composite control, on the other hand, eliminates endpoint vibrations in a settling time of 1.5 seconds, while reducing the large initial undershoot to 5°.

6. Conclusion

This article has addressed the endpoint position control problem for a two-link flexible mechanism with very flexible links. Motivated by the success of application to a single rotating flexible link experiment [17], the approach applied in this study is a two-stage, or composite control strategy that employs input shaping in conjunction with the post-slew feedback scheme. A derivation of the input shaping prefilter indicates the role of the precompensation scheme in the frequency domain, and results in application are relatively good for a range of maneuvers. If one considers the nonlinear plant over a range of operating points, about which the system may be linearized, ARMA model-based schemes may be

employed for the post-slew vibration control, either in a fixed or adaptive controller setting. The implemented controllers were designed based on the simplified assumption of independent joint control, utilizing output feedback from the endpoint acceleration and the joint position. The controller performance was found to be satisfactory for small parameter variations (changes in modal frequencies), in terms of settling time and endpoint vibration suppression. Combining the two stages of the control, then, has given rise to the composite strategy, which benefits from the fast slew capabilities of the input shaping with minimal residual vibration, as well as from the disturbance rejection properties of the feedback control.

Input shaping, in which the impulse sequences are designed for a nominal operating frequency, can be used in several extensions along these lines, such as in an adaptive setting [18] or as an additional loop in force control applications for flexible link systems [20]. Furthermore, given that the performance of the controllers described here degrades when a load is applied at the endpoint, a self-tuning approach is advocated to resolve the robustness of the closed-loop system with respect to inherent system parameter changes. Work is currently continuing along those lines, and some of those results have appeared in [11] and [21]. Those references, as well as [12], also serve to complement, from an analytical viewpoint, the experimental results reported on in this article.

Acknowledgments

The authors gratefully acknowledge the contributions of Dr. Anthony P. Tzes and Erick R. Garcia-Benitez for assistance in this ongoing effort.

References

1. S. Yurkovich and F.E. Pacheco, "On controller tuning for a flexible-link manipulator with varying payload," *J. Robot. Syst.*, vol. 6, no. 3, pp. 233-254, June 1989.
2. S. Yurkovich, F.E. Pacheco, and A.P. Tzes, "On-line frequency domain information for control of a flexible-link robot with varying payload," *IEEE Trans. Automat. Control*, vol. AC-33, no. 12, pp. 1300-1303, 1989.
3. S. Yurkovich and A.P. Tzes, "Experiments in the identification and control of flexible-link manipulators," *IEEE Control Syst.*, vol. 10, no. 2, pp. 41-47, 1990.
4. A. Tzes and S. Yurkovich, "Application and comparison of on-line identification methods for flexible manipulator control," *Int. J. Robot. Re.*, vol. 10, no. 5, pp. 515-527, 1991.
5. D.M. Rovner and R.C. Cannon, "Experiments toward on-line identification and control of a very flexible one-link manipulator," *Int. J. Robot. Re.*, vol. 6, no. 4, pp. 3-19, 1987.
6. D.M. Rovner and G.F. Franklin, "Experiments in load-adaptive control of a very flexible one-link manipulator," *Automatica*, vol. 24, no. 4, pp. 541-548, 1988.
7. E. Schmitz, "Modeling and control of a planar manipulator with an elastic forearm," in *Proc. IEEE Int. Conf. Robot. Automat.*, pp. 894-899, Scottsdale, AR, May 1989.
8. C.M. Oakley and R.C. Cannon, "End-point control of a two-link manipulator with a very flexible forearm: Issues and experiments," in *Proc. Am. Control Conf.*, pp. 1381-1388, Pittsburgh, PA, June 1989.
9. V. Feliu, K.S. Rattan, and H.B. Brown, "Adaptive control of a single-link flexible manipulator in the presence of joint friction and load changes," in *Proc. IEEE Int. Conf. Robot. Automat.*, pp. 1036-1041, Scottsdale, AR, May 1989.

10. H. Krishnan and M. Vidyasagar, "Control of a single-link flexible beam using a Hankel-norm-based reduced order model," in *Proc. IEEE Int. Conf. Robot. Automat.*, pp. 9–14, Philadelphia, PA, April 1988.
11. S. Yurkovich, A.P. Tzes, I. Lee, and K.L. Hillsley, "Control and system identification of a two-link flexible manipulator," in *Proc. IEEE Int. Conf. Robot. Automat.*, pp. 1626–1631, Cincinnati, OH, May 1990.
12. S. Yurkovich, A.P. Tzes, and K.L. Hillsley, "Controlling coupled flexible links rotating in the horizontal plane," in *Proc. Am. Control Conf.*, pp. 362–367, San Diego, CA, June 1990.
13. P. Mechkl and W. Seering, "Feedforward control techniques to achieve fast settling time in robots," in *Proc. Am. Control Conf.*, Seattle, June 1986.
14. N.C. Singer and W.P. Seering, "Preshaping command inputs to reduce system vibration," Technical Report A.I. Memo No. 1027, MIT Artificial Intelligence Laboratory, Cambridge, MA, 1988.
15. N.C. Singer and W.P. Seering, "Using acausal shaping techniques to reduce robot vibrations," in *Proc. IEEE Int. Conf. Robot. Automat.*, pp. 1434–1439, Philadelphia, PA, April 1988.
16. N.C. Singer and W.P. Seering, "Preshaping command inputs to reduce system vibration," *Trans. ASME J. Dyn. Meas. Control*, vol. 112, no. 1, pp. 76–82, 1990.
17. A. Tzes, M. Englehart, and S. Yurkovich, "Input preshaping with frequency domain information for flexible-link manipulator control," in *Proc. AIAA Guidance, Navigation Control Conf.*, Boston, MA, August 1989.
18. A. Tzes and S. Yurkovich, "An adaptive input shaping control scheme for vibration suppression in slewing flexible structures," *IEEE Trans. Control Sys. Tech.*, vol. 1, no. 2, June 1993.
19. P. Kotnik, S. Yurkovich, and U. Özgüner, "Acceleration feedback for control of a flexible manipulator arm," *J. Robot. Syst.*, vol. 5, no. 3, pp. 181–196, 1988.
20. A. Tzes and S. Yurkovich, "Flexible link manipulator force control," in *Proc. Am. Control Conf.*, pp. 194–199, San Diego, CA, 1990.
21. S. Yurkovich, A.P. Tzes, and K.L. Hillsley, "Identification and control for a manipulator with two flexible links," in *Proc. IEEE Conf. Decision Control*, Honolulu, HI, December 1990.